

Short Communication

Metabolism of Ketoconazole and Deacetylated Ketoconazole by Rat Hepatic Microsomes and Flavin-Containing Monoxygenases

ABSTRACT:

Ketoconazole (KT) has been reported to cause hepatotoxicity, which is probably not mediated through an immunological mechanism. Although KT is extensively metabolized by hepatic microsomal enzymes, the nature, route of formation, and toxicity of suspected metabolites are largely unknown. Recent reports indicate that *N*-deacetyl ketoconazole (DAK) is a major initial metabolite in mice, which, like lipophilic 4-alkylpiperazines, is susceptible to successive oxidative attacks on the N-1 position producing ring-opened dialdehydes. The rate of formation of DAK from hepatic rat microsomal incubations of KT was determined by HPLC. The rate of disappearance for KT was almost equal to the rate of DAK formation: 5.96 and 5.88 $\mu\text{M}/\text{hr}$, respectively. Also, the potential bioactivation of DAK was evaluated by measuring substrate activity of DAK with purified pig liver flavin-containing monoxy-

genase (FMO) and rat liver microsomes. Activity was measured by following DAK-dependent oxygen uptake polarographically at 37°C in pyrophosphate buffer (pH 8.8) containing the glucose-6-phosphate NADPH-generating system. The K_M 's of DAK were 34.6 and 77.4 μM for the purified FMO and rat microsomal FMO, respectively. Lastly, DAK was found to be metabolized by an NADPH-dependent rat liver microsomal monoxygenases at pH 8.8 to two metabolites as determined by HPLC. Heat inactivation of rat liver microsomal FMO abolished the formation of these metabolites from DAK. SKF-525A and anti-rat NADPH cytochrome P450 reductase did not inhibit this reaction. These results suggest that deacetylation of KT yields a major product, DAK, for further metabolism by microsomal monoxygenases that seem to be FMO-related.

KT¹ was the first oral antifungal agent in a series of azole derivatives with a broad spectrum of activity against systemic mycotic infections. KT and other azoles, fluconazole and itraconazole, have become prominent broad spectrum oral antifungal agents in the treatment of systemic mycoses, especially in patients with the acquired immune deficiency syndrome. KT exerts its antifungal actions by blocking the conversion of lanosterol or 24-methylene-dihydrolanosterol to ergosterol in fungi (1). Also, KT has been shown to inhibit a number of CYP enzymes involved in steroidogenesis and drug metabolism (2, 3), which has allowed KT to be used for the treatment of androgen-dependent diseases such as prostate cancer (4).

Therapeutic concentrations, dosages, and duration of treatment of KT vary depending on the medical diagnosis. The mean peak serum concentration in humans after a 200 mg/day dose of KT ranges from 8 to 19 μM (5, 6) and from 13 to 26 μM after a 400 mg/day dose (7). Moreover, KT concentrations have been reported to be as high as 94 μM in humans (8). In rats, 10 and 20 mg/kg KT doses resulted in peak plasma levels of 24 and 62 μM KT, respectively (9). Thus, the mean peak plasma concentrations vary according to dosage. The distribution of KT and metabolites after oral administration in rats has been shown to be concentrated in the liver at higher concentrations than plasma (9). Specific tissue binding of KT in hepatic microsomal fractions from the rat was 89% (10). Thus, the binding of KT to rat liver microsomes may result in potent inhibition of mixed function oxida-

tive metabolism *in vivo* and *in vitro*.

The half-life of KT seems to be dose-dependent, increasing with increasing dose and after repeated dosing (6, 9). The slower elimination phase is also dose-dependent. Thus, long-term administration of KT can result in drug accumulation in humans (5), in rats and dogs (9), and in mice (11). The increasing dose-dependent half-life during long-term treatment in humans suggests autoinhibition of metabolism (5). Furthermore, KT displays nonlinear kinetics in both the volume of distribution and clearance as the dose is escalated (6). These observations correlate with the first-pass elimination of KT, with transient saturation of the drug-metabolizing capacity of the liver at higher dosages (5, 6, 9). Also, KT has been purported to be extensively metabolized to a large number of metabolites, with hepatic microsomal enzymes playing the major role in the biotransformation reactions (9, 10). The metabolic pathways suggested in KT's biotransformation include oxidation, cleavage, degradation, and scission of the imidazole and piperazine rings, oxidative *O*-dealkylation, and aromatic hydroxylation (5, 9, 12). *N*-deacetyl ketoconazole (DAK), Fig. 1, appears to be the major metabolite reported in mice (11). Also, accumulation of KT in mouse liver was minimal, whereas the hepatic levels of DAK were significant (13).

There have been numerous documented cases of KT-induced hepatitis (14, 15). Many reports indicate that the type of hepatic injury is zone 3 necrosis (14, 15). Presently, the mechanism of KT-induced hepatotoxicity is unknown. The absence of the clinical manifestation of hypersensitivity and eosinophil-rich infiltration or granulomas in liver biopsy suggests that the liver lesion might be related to a direct or a reactive metabolite (14, 15). The aims of this present study were to investigate KT's and DAK's metabolism using postnatal rat microsomes. These studies evaluated the rate of formation of DAK from postnatal rat hepatic microsomes incubated with KT by HPLC; the potential bioactivation of DAK by FMO using purified pig liver FMO

Received October 1, 1996; accepted February 21, 1997.

¹ Abbreviations used are: KT, ketoconazole; CYP, cytochrome P450; DAK, *N*-deacetyl ketoconazole; FMO, flavin-containing monoxygenase; CL, clotrimazole; IgG, immunoglobulin G.

Send reprint requests to: Dr. Daniel Acosta, Jr., College of Pharmacy, Office of the Dean, University of Cincinnati, P.O. Box 670004, Cincinnati, OH 45267-0004.

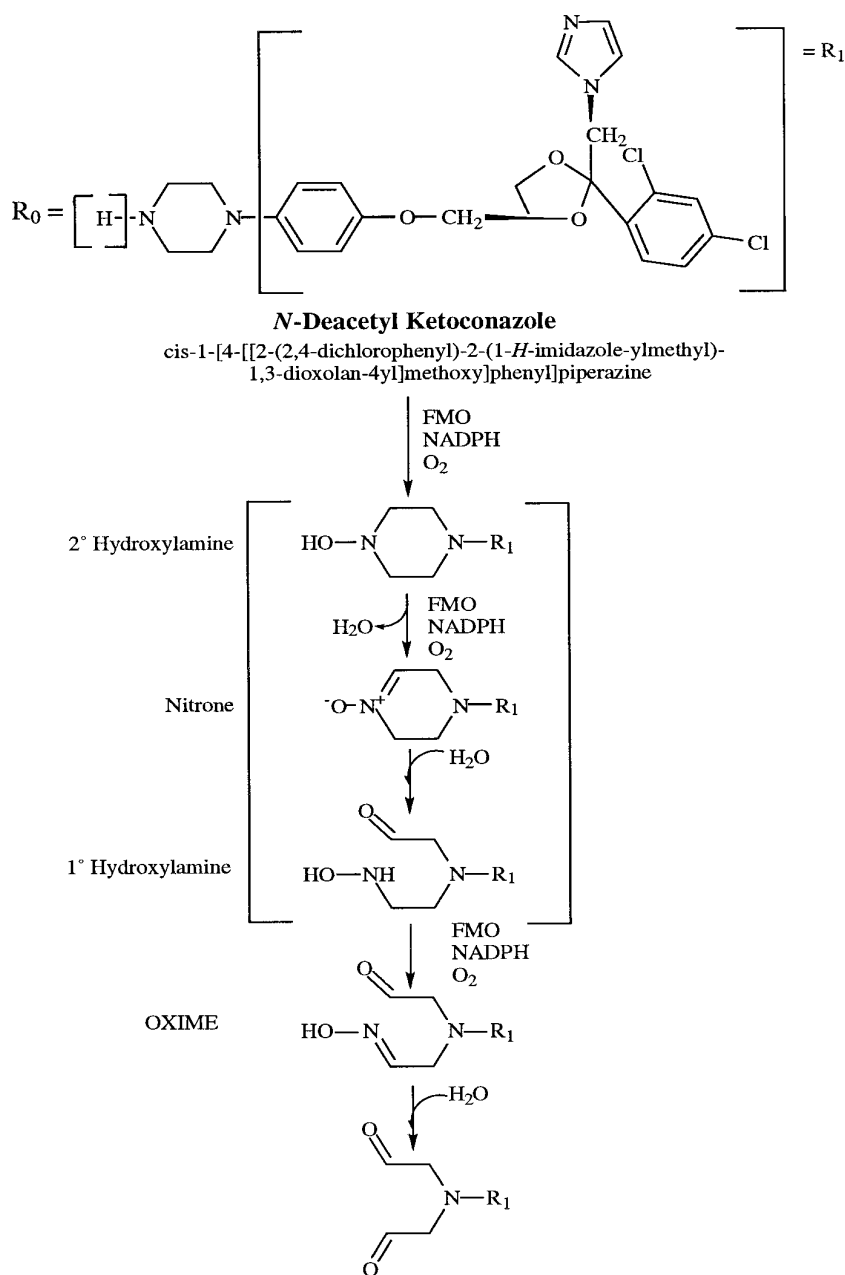


FIG. 1. Proposed metabolic pathway of DAK by FMOs to reactive metabolites.

Ketoconazole: $R_0 = -\text{COCH}_3$.

and postnatal rat hepatic microsomal-FMO; and the NADPH-dependent rat liver microsomal metabolism of DAK *in vitro*.

Materials and Methods

Chemicals. Glucose-6-phosphate, glucose-6-phosphate dehydrogenase, and methimazole were from Sigma Chemical Co. (St. Louis, MO). *n*-Octylamine was purchased from Eastman Organic Chemicals (Rochester, NY). Purified pig liver FMO was a generous gift from Dr. D. Ziegler (Austin, TX). KT and DAK were generous gifts from Janssen Pharmaceutical (Beerse, Belgium). All other reagents were the highest available purity from commercial sources. Solvents used for HPLC analysis were HPLC grade.

Isolation of Postnatal Rat Liver Microsomes. The liver tissues were removed from 8- to 10-day-old Sprague-Dawley rats and immediately placed on ice. Tissues were homogenized with 0.25 M sucrose, 100 mM Trizma, and 1 mM EDTA (pH 7.5). Microsomes were prepared by standard differential

centrifugation and stored in 10 mM Trizma, 1 mM EDTA, and 20% glycerol (pH 7.5). Samples were frozen in liquid nitrogen and stored at -80°C . Protein was determined using the Biorad Assay.

Extraction of KT and DAK from Hepatic Microsomes. One-milliliter aliquots were obtained from microsomes (2 mg microsomal protein/ml) incubated with 100 μM KT in 0.05 M KH_2PO_4 buffer (pH 7.4) at 37°C . These aliquots were spiked with 180 μM as the internal standard. KT and DAK were extracted from the microsomal preparations with 3 ml ether (pH 9.0). Ether extractions were pooled and evaporated under nitrogen gas to dryness. The pellet was redissolved in 125 μl mobile phase and then injected into the HPLC column.

HPLC. HPLC analysis for the deacetylation of DAK from KT was conducted using an Analytical Science, Inc., C_{18} column (Santa Clara, CA) connected to a Waters 600E system controller, a Waters 486 tunable absorbance detector, and a Waters 700 satellite WISP. The column was eluted with

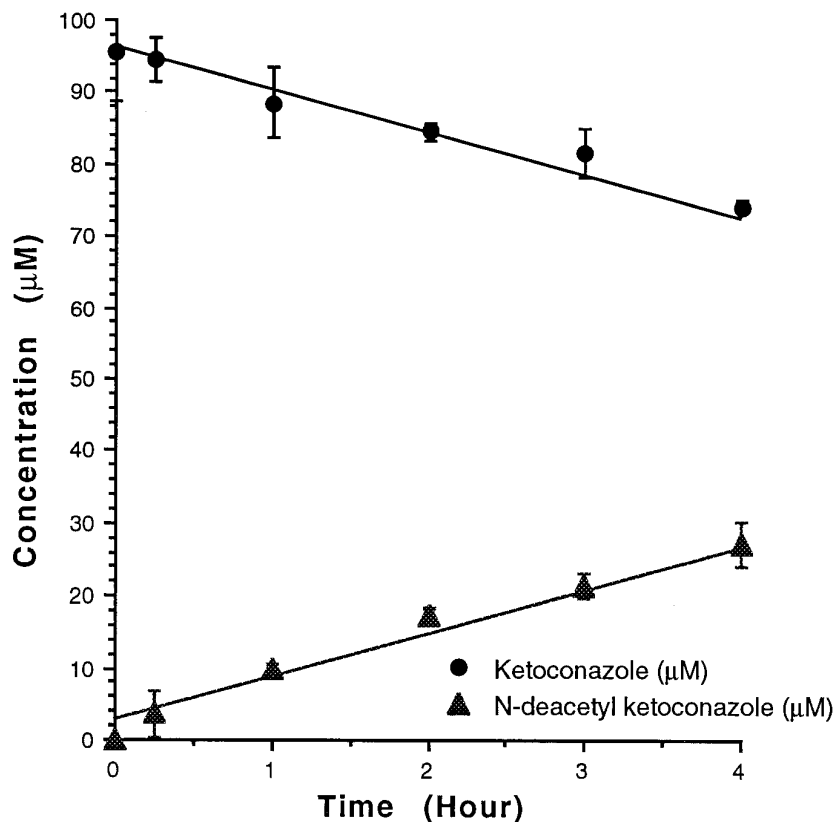


FIG. 2. Formation of DAK and disappearance of KT after postnatal rat microsomal incubation of 100 μM KT in 0.05 M KH_2PO_4 buffer (pH 7.4) at 37°C.

Error bars represent the standard deviation of three separate experiments.

water:methanol:0.1% triethylamine (25:75:0.1, v/v) at a flow rate of 2.0 ml/min. The wavelength was set at 254 nm. HPLC analysis for the evaluation of DAK's metabolism was performed with a Beckman (Fullerton, CA) system (two model 110A pumps and an Altex model 420 controller/programmer) and a Hewlett-Packard (Palo Alto, CA) model 1040A diode array detector. DAK and its metabolites were resolved on a 4.1 \times 250 mm Hamilton PRP-1 reversed-phase column (Reno, NV) eluted with 0.005 M ammonium formate (pH 5.6) and 30–60% acetonitrile at a flow rate of 1.5 ml/min, with a detection at 220 nm.

Standard curves were generated for quantifying KT and DAK. A total of 0, 12.5, 25, 50, 75, and 100 μl of 1 mM KT and 0, 12.5, 25, 50, and 75 μl of 1 mM DAK were placed in glass test tubes. The solvent was evaporated under nitrogen gas. One-milliliter of 0.05 M potassium phosphate buffer (pH 9.0), 180 μM CL, and 3 ml ether were added. The tubes were capped, mixed by inversion for 30 min, and centrifuged. The organic layer was removed and evaporated under nitrogen gas. Samples were reconstituted in 125 μl mobile phase. Resultant peak areas were used to generate standard curves for KT as peak area ratio (KT/CL) versus [KT] and DAK as peak area ratio (DAK/CL) versus [DAK]. Unknown values were determined by extraction and analysis as described previously, followed by interpolation using these standard curves that were performed in duplicate.

Metabolic Assays. Reactions catalyzed by purified pig FMO and microsomal-FMO were conducted polarographically at 37°C in 0.1 M glycine:25 mM pyrophosphate buffer (pH 8.8), containing the glucose-6-phosphate NADPH generating system. The NADPH generating system consisted of 250 μM NADP⁺, 1.25 mM glucose-6-phosphate, and 1 unit/ml glucose-6-phosphate dehydrogenase. Also, 5 mM octylamine, a known positive effector for FMO, as well as an inhibitor of CYP (16), was present in the incubation chamber. After 3–4 min temperature equilibration, the reaction was started by adding the hepatic microsomes (3 mg/ml) or purified pig liver FMO to the oxygen chamber. After a blank rate was obtained, various concentrations of DAK (25, 50, 75, 100, 150, and 200 μM) were added to the chamber. Controls with 1.25 mM methimazole were performed with purified FMO and microsomes.

In vitro metabolism of DAK by microsomes from postnatal rat liver was a modified procedure of Miranda *et al.* (17). The incubation mixture consisted of 1.5 mg microsomal protein, 0.1 M glycine:25 mM pyrophosphate buffer (pH 8.8), 100 μM DAK, 3 mM octylamine, and the NADPH-generating system (10 mM glucose-6-phosphate, 1.0 unit/ml glucose-6-phosphate dehydrogenase, and 1 mM NADP⁺) in a total volume of 0.5 ml. After 1-hr incubation at 37°C with shaking, the reaction was terminated with 0.5 ml of ice-cold methanol, cooled on ice, and pH adjusted to 5 with 1 N HCl. Proteins were precipitated by centrifugation at 14,000g for 20 min at 4°C, and aliquots of the supernatant were analyzed by HPLC as described. When anti-rat NADPH CYP reductase IgG was used to inhibit the CYP microsomal enzyme activity, the IgG (6 mg IgG/mg microsomal protein) and microsomes were preincubated for 20 min at 25°C before the addition of other components. To determine the effect of heat treatment on FMO activity, microsomes were heated at 50°C for 90 sec before adding them to the incubation mixture. To evaluate CYP metabolism of DAK, the microsomes were added to an incubation mixture consisting of 0.1 M phosphate buffer (pH 7.4), 100 μM DAK, and the NADPH-generating system.

Results and Discussion

Because KT has been reported to be primarily metabolized in the liver by oxidation of the imidazole ring, degradation of the oxidized imidazole, oxidative *O*-dealkylation, oxidative degradation of the piperazine ring, and aromatic hydroxylation to a large number of metabolites (5, 9), further metabolic and toxicity investigations may help explain their role, if any, in KT's toxicity. Our earlier studies revealed that DAK was more cytotoxic than KT in a distinct time- and dose-response relationship using postnatal rat hepatocytes, thus suggesting that bioactivation of DAK may be responsible for the observed hepatotoxicity (18). Also, DAK's toxicity was enhanced with octylamine and suppressed with methimazole, thus suggesting that FMO may play a role in KT's hepatotoxicity (18). Moreover, DAK,

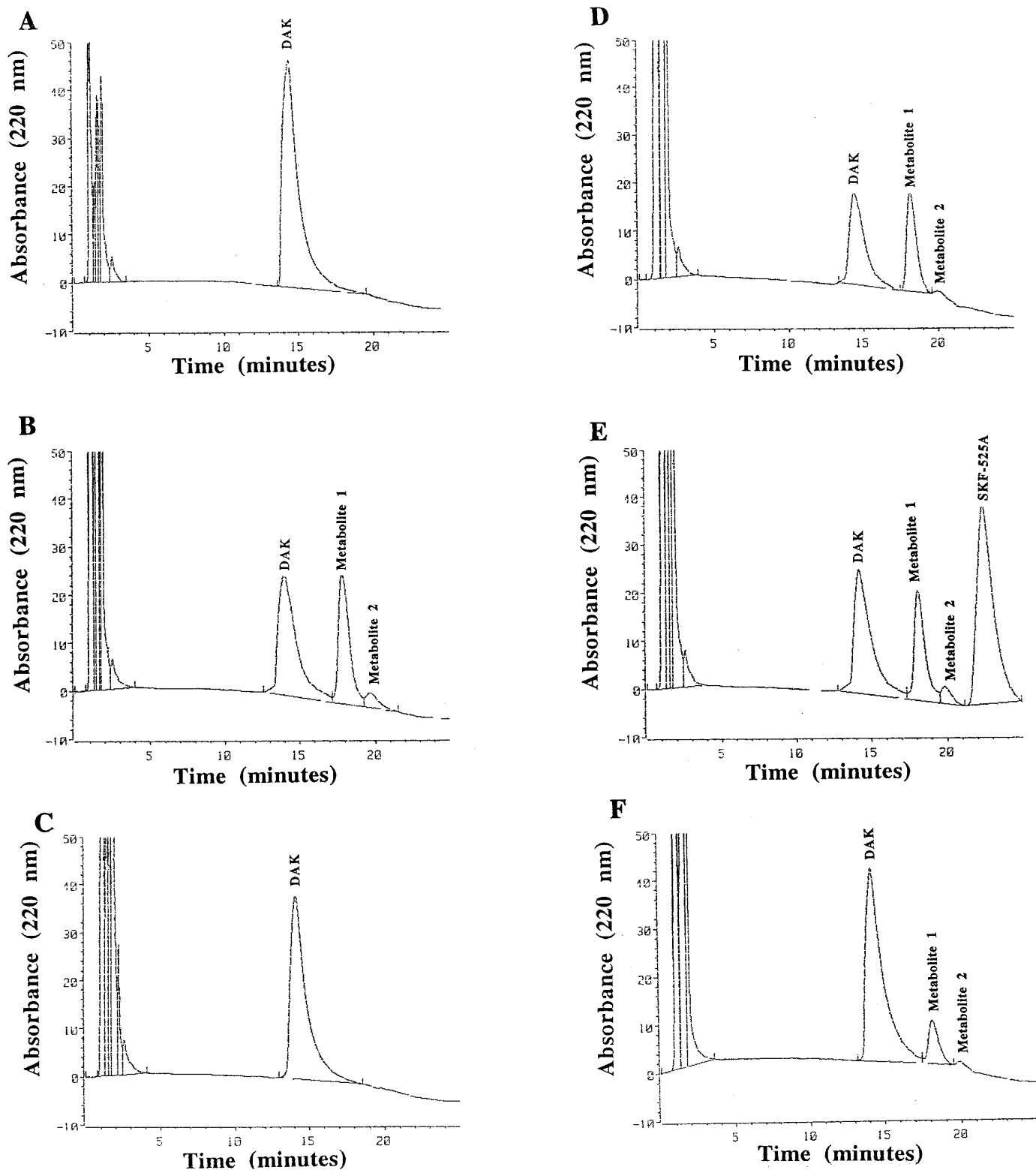


FIG. 3. HPLC of DAK's metabolism using postnatal rat hepatic microsomes.

(A) No NADPH-generating system (pH 8.8). (B) NADPH-generating system (pH 8.8). (C) FMO heat inactivation, 50°C for 90 sec; NADPH-generating system (pH 8.8). (D) NADPH-generating system with anti-rat NADPH CYP reductase (6 mg IgG/mg microsomal protein; pH 8.8). (E) NADPH-generating system with SKF-525A (0.5 mM; pH 8.8). (F) NADPH-generating system (pH 7.4) in 0.1 M phosphate buffer.

like lipophilic 4-alkylpiperazines, is susceptible to successive oxidative attacks by FMO on the N-1 position, which may produce potentially toxic ring-opened dialdehydes (fig. 1). The intermediate metabolites, primary and secondary hydroxylamines, which would be formed by the proposed pathway, are also substrates for FMO. Therefore, the increased susceptibility of the liver cells to the deacetylated compound may be a result of its metabolism by FMO to a toxic metabolite.

Because of the aforementioned studies, DAK may be responsible, in part, for the observed hepatotoxicity of KT. Also, the delayed onset of toxicity of KT *versus* DAK in earlier studies may be due to a rate-limiting step such as deacetylation. Under the HPLC conditions previously mentioned, the following retention times were observed: KT, 3.25 min; CL, 3.98 min; and DAK, 9.47 min. The standard curves of the peak area ratios were obtained by linear regression. Our results demonstrate that the rate of DAK formation and the rate of KT disappearance followed zero-order kinetics, with correlations of 0.988 and 0.976 for KT and DAK, respectively. The rate of disappearance ($5.96 \mu\text{M/hr}$) for KT was almost equal to the rate of DAK formation ($5.88 \mu\text{M/hr}$; fig. 2). These results suggest that DAK was formed from KT in postnatal rat hepatic microsomes. Therefore, it is possible when cofactors that are necessary for oxidative metabolism are present in an *in vivo* or *in vitro* system, the deacetylated metabolite of KT may form potentially toxic or reactive metabolite(s).

The absence of hypersensitivity after KT's administration suggests that the liver lesion might be related to a direct or a reactive metabolite (14, 15). Moreover, the increased susceptibility of the liver cells to DAK in comparison to KT may also be suggestive of metabolism to a reactive metabolite (18). The K_M 's for DAK with the purified pig liver FMO enzyme preparations and the microsomal FMO preparations were calculated from double reciprocal plots of velocity *versus* substrate concentration above and below K_M . The K_M 's for DAK were 34.6 ± 6.4 and $77.4 \pm 0.8 \mu\text{M}$ for the purified FMO and the postnatal rat microsomal FMO, respectively. Results were mean values from 3 to 4 experiments. The purified enzyme was used as a positive control to observe FMO substrate activity with DAK. The results demonstrated that DAK was an excellent substrate for the purified pig liver FMO and the postnatal hepatic microsomal-FMO. These data suggest that DAK is further metabolized by FMO to form metabolite(s) that may ultimately play a role in KT's toxicity.

Our last aim was to evaluate DAK's metabolism by NADPH-dependent monooxygenases using hepatic postnatal rat microsomes so that we can correlate the results to our previous studies. Figure 3 demonstrates the results of DAK's metabolism from postnatal microsomal incubations. The retention times were: DAK, 14.2 min; metabolite 1 (major), 18.1 min; and metabolite 2 (minor), 19.8 min. Figure 3A does not contain the NADPH-generating system resulting in no metabolite formation. Figure 3B demonstrates that two metabolites were produced after microsomal oxidative metabolism of DAK. These metabolite peaks were not formed when the liver microsomal FMO was heat-inactivated (fig. 3C). Figure 3 (D and E) used SFK-525A and anti-rat NADPH IgG reductase to inhibit microsomal CYP in the incubation mixture. The inhibitors had minimal effect on DAK's metabolism. Figure 3F demonstrates that DAK was minimally metabolized at pH 7.4. These results suggest that DAK is primarily converted to metabolites 1 and 2 by FMO and not by CYP in the postnatal rat liver microsomes.

We propose that bioactivation of DAK by successive oxidative attacks by FMO on the piperazine ring may generate primary or secondary hydroxylamines. These amines may also serve as substrates of FMO eventually forming a ring-opened dialdehyde that could result

in toxic consequences (fig. 1). To date, none of our proposed metabolites in the metabolism of DAK by FMO have been reported in the literature; however, we are currently isolating and identifying DAK's metabolites (1 and 2) apparently generated by FMO. Other metabolites may have been formed from DAK that were not detected by the HPLC method used in the present study. Also, Whitehouse *et al.* (19) have isolated and identified two metabolites of KT from mouse liver that were *N*-oxides. The formation of these metabolites seemed to be minute quantities in comparison with KT or DAK. The formation of *N*-oxide's is presumptive evidence for the role of FMO in the metabolism of a specific xenobiotic amine (20). The reduction of metabolically generated *N*-oxides by the enzymes present in different cell compartments will limit their release from the liver (21). Furthermore, if both oxidation and reduction reactions occur rapidly, tissue NADPH concentrations may be perturbed (21). NADPH could be depleted during the metabolism of DAK to metabolites 1 and 2. Loss of cellular NADPH would affect a number of cellular processes and may be responsible, in part, for the toxicity of some tertiary amines (21). Thus, it is possible that, in addition to DAK's metabolism by FMO, the *N*-oxide's of KT—*cis*-1-acetyl-4-[4-[[2-(2,4-dichlorophenyl)-2-(1*H*-4,5-dihydroimidazol-1-yl-methyl)-1,3-dioxolan-4-yl]methoxy]phenyl]piperazine-4-oxide and *cis*-1-acetyl-4-[4-[[2-(2,4-dichlorophenyl)-2-(*N*-formyl-*N*-(2-aminoethylene)-amino-methyl)-1,3-dioxolan-4-yl]-methoxy]-phenyl]piperazine-4-oxide—may also play a role in the hepatotoxicity of KT. In either situation, FMO seems to play a role in the metabolism of KT and DAK.

Department of Pharmacology/Toxicology,
College of Pharmacy,
University of Texas at Austin (D.A.);
and College of Pharmacy,
Oregon State University (R.J.R.)

ROSITA J. RODRIGUEZ
DANIEL ACOSTA, JR.

References

1. H. Vanden Bossche, P. Marichal, J. Gorrens, H. Geerts, and P. A. Janssen: Basis for the search for new antifungal drugs. *Ann. N.Y. Acad. Sci.* **544**, 191–207 (1988).
2. J. J. Sheets and J. I. Mason: Ketoconazole: a potent inhibitor of cytochrome P-450-dependent drug metabolism in rat liver. *Drug Metab. Dispos.* **12**, 603–606 (1984).
3. C. G. Meredith, A. L. Maldonado, and K. V. Speeg: The effect of ketoconazole on hepatic oxidative drug metabolism in the rat *in vivo* and *in vitro*. *Drug Metab. Dispos.* **13**, 156–162 (1985).
4. A. Pont, J. R. Graybill, P. C. Craven, J. N. Galgiani, W. E. Dismukes, R. E. Reitz, and D. A. Stevens: High-dose ketoconazole therapy and adrenal and testicular function in humans. *Arch. Intern. Med.* **144**, 2150–2153 (1984).
5. R. C. Heel, R. N. Brogden, A. Carmine, P. A. Morley, T. M. Speight, and G. S. Avery: Ketoconazole: a review of its therapeutic efficacy in superficial and systemic fungal infections. *Drugs* **23**, 1–36 (1982).
6. Y. C. Huang, J. L. Colaizzi, R. H. Bierman, R. Woestenborghs, and J. Heykants: Pharmacokinetics and dose proportionality of ketoconazole in normal volunteers. *Antimicrob. Agents Chemother.* **30**, 206–210 (1986).
7. J. G. Baxter, C. Brass, J. Schentag, and R. Slaughter: Pharmacokinetics of ketoconazole administered intravenously to dogs and orally as tablet and solution to humans and dogs. *J. Pharmaceut. Sci.* **75**, 443–447 (1986).
8. A. M. Sugar, S. G. Alsip, J. N. Galgiani, J. R. Graybill, W. E. Dismukes, G. Cloud, P. Craven, and D. Stevens: Pharmacology and toxicity of high-dose ketoconazole. *Antimicrob. Agents Chemother.* **31**, 1874–1878 (1987).

9. E. W. Gascoigne, G. J. Barton, M. Michaels, W. Meuldermans, and J. Heykants: The kinetics of ketoconazole in animals and man. *Clin. Res. Rev.* **1**, 177–187 (1981).
10. T. Daneshmend and D. Warnock: Clinical pharmacokinetics of ketoconazole. *Clin. Pharmacokinet.* **14**, 13–34 (1988).
11. L. W. Whitehouse, A. Menzies, B. Dawson, J. Zamecnik, and W. W. Sy: Deacetylated ketoconazole: a major ketoconazole metabolite isolated from mouse liver. *J. Pharmaceut. Biomed. Anal.* **8**, 603–606 (1990).
12. G. Medoff and G. S. Kobayashi: Strategies in the treatment of systemic fungal infections. *N. Engl. J. Med.* **302**, 145–155 (1980).
13. L. W. Whitehouse, A. Menzies, R. Mueller, and R. Pontefract: Ketoconazole-induced hepatic phospholipidosis in the mouse and its association with de-N-acetyl ketoconazole. *Toxicology* **94**, 81–95 (1994).
14. G. Lake-Bakaar, P. J. Scheuer, and S. Sherlock: Hepatic reactions associated with ketoconazole in the United Kingdom. *Br. Med. J.* **294**, 419–422 (1987).
15. B. H. C. Stricker, A. P. R. Blok, F. B. Bronkhorst, G. E. Van Parys, and V. J. Desmet: Ketoconazole-associated hepatic injury a clinicopathological study of 55 cases. *J. Hepatol.* **3**, 399–406 (1986).
16. J. R. Cashman and D. M. Ziegler: Contribution of N-oxygenation to the metabolism of MPTP (1-methyl-4-phenyl-1,2,3,6-tetrahydropyridine) by various liver preparations. *Mol. Pharmacol.* **29**, 163–167 (1986).
17. C. Miranda, W. Chung, R. Reed, X. Zhao, M. Henderson, J. Wang, D. Williams, and D. Buhler: Flavin-containing monooxygenase: a major detoxifying enzyme for the pyrrolizidine alkaloid senecionine in guinea pig tissues. *Biochem. Biophys. Res. Comm.* **178**, 546–552 (1991).
18. R. J. Rodriguez and D. Acosta: N-deacetyl ketoconazole-induced hepatotoxicity in a primary culture system of rat hepatocytes. *Toxicology* **117**, 123–131 (1997).
19. L. W. Whitehouse, A. Menzies, B. Dawson, T. Cyr, A. By, D. Black, and J. Zamecnik: Mouse hepatic metabolites of ketoconazole: isolation and structure elucidation. *J. Pharmaceut. Biomed. Anal.* **12**, 1425–1441 (1994).
20. D. M. Ziegler: Recent studies on the structure and function of multisubstrate flavin-containing monooxygenases. *Ann. Rev. Pharmacol. Toxicol.* **33**, 179–199 (1993).
21. D. M. Ziegler: Flavin-containing monooxygenases: catalytic mechanism and substrate specificities. *Drug Metab. Rev.* **19**, 1–32 (1988).